35th Annual International Conference of the IEEE EMBS
Osaka, Japan, 3 - 7 July, 2013

Simulating Cell Apoptosis Induced Sinus Node Dysfunction*

Sanjay Kharche, John Beling, Irina V Biktasheva, Henggui Zhang, and Vadim N Biktashev

Abstract— **Sinus node dysfunction (SND) is correlated to the pacemaker sinoatrial node (SAN) cell apoptosis. This study explores the effect of such a dysfunctional SAN on electrical propagation into neighboring atrial tissue.**

The Fenton Karma model was extended to simulate mouse SAN and atrial cell action potentials. The cell models were incorporated into a 2D model consisting of a central SAN region surrounded by atrial tissue. The intercellular gap junctional coupling, as quantified by the diffusion constant, was estimated to give conduction speeds as observed in mouse atrial tissue. The size of mouse SAN pacemaking region was estimated using the 2D model. In multiple simulations, the effects of an increasing proportion of apoptotic pacemaker cells on atrial tissue pacing were simulated and quantified.

The SAN size that gave a basal mouse atrial cycle length (ACL) of 295 ms was found to be 0.6 mm in radius. At low pacemaker cell apoptosis proportion, there was a drastic increase of ACL. At modest increase in the number of apoptotic cells, bradycardia was observed. The incidence of sinus arrest was also found to be high. When the number of apoptotic cells were 10% of the total number of pacemaking cells, all pacemaking was arrested.

Phenomenological models have been developed to study mouse atrial electrophysiology and confirm experimental findings. The results show the significance of cell apoptosis as a major mechanism of SND.

I. Introduction

The sino-atrial node (SAN) is the primary pacemaker of the heart and SAN dysfunction (SND) is known to give rise to bradycardia, sinus arrest, and sinus pause [1]. The mouse is a popular experimental model in the study of clinical arrhythmia, including SND. Intracellular mechanisms regulating electrical pacemaking of mouse SAN cells have been studied in detail experimentally [2, 3] and quantified into mathematical models [4]. It is established that SAN pacemaking is strongly regulated by an intra-cellular calcium (Ca^{2+}) clock [4, 5]. A recent study [6] has identified that stress and hypertension abnormally raise levels of Ca^{2+}/calmodulin-dependent protein kinase II (CamKII), an important factor in pacemaking mechanisms. Such pathologically high levels of CamKII have been found to cause pacemaker cell death, or cell apoptosis. In this study, we consider the tissue level pacemaking function of a heterogeneous SAN consisting of normal pacemaker cells as well as apoptotic cells. Computationally efficient phenomenological models were favored over biophysical models to simulate the electrophysiological excitation in a spatially extended 2D model. This allowed rapid model development and facilitated multiple simulations required to give conclusive simulation experiment results. The aims of this study were: (i) to develop phenomenological models of excitation for mouse SAN and atrial action potentials (APs) based on the Fenton Karma (FK) model [7]; (ii) to computationally estimate the SAN region size using the modified FK models and idealized 2D tissue preparations; and (iii) to quantify the occurrence of bradycardia and sinus exit block due to cell apoptosis in the SAN region.

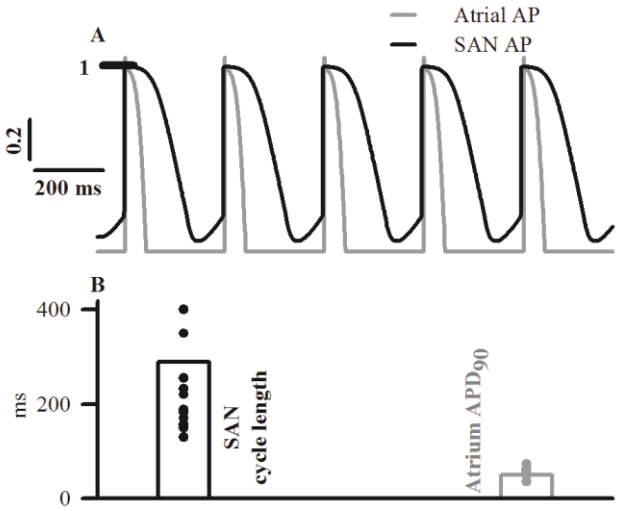

Fig 1. Simulated APs using the modified FK models. A: AP profiles of mouse SAN (solid line) and mouse atrial (gray line) cell types. B: Validation of SAN cycle length and atrial APD_{90}. Symbols show experimental data and bars show simulation results.

The computational cardiology simulation environment, Beatbox [8] was used to develop and construct all simulation models for this study.

II. Methods

The 3 variable FK model [7] for cardiac excitation was adopted in this study. The FK model consists of three simplified currents: fast inward, slow inward, and slow outward current. It *quantitatively* approximates the restitution properties and spiral wave behaviour of detailed ionic models of cardiac action potential. In this study, we modified the original FK model by adding hyperpolarization-activated current, J_h, using the following formulation:

*This work is supported by EPSRC (UK) grants (EP/I029664/1, EP/I029826/1, EP/I030158/1), PRACE Introductory HPC Access (PRPB09, 2012). The calculations for this paper were performed using HECToR UK national supercomputing facility and the University of Exeter Supercomputer.

S Kharche and V N Biktashev are with CEMPS, University of Exeter, Exeter, UK. (phone: 01392 726636; e-mail: S.R.Kharche@exeter.ac.uk).

H Zhang and J Beling are with Biological Physics, Physics Department, University of Manchester, Manchester, M13 9PL, UK.

I V Biktasheva is with Computer Science Department, University of Liverpool, Liverpool, L69 3BX, UK.

$$
\begin{aligned}
\partial u/\partial t &= D\nabla^2 u - J_{fi} - J_{so} - J_{si} - J_h \\
\partial v/\partial t &= \Theta(u_c - u)(1-v)\tau_v^- - \Theta(u-u_c)v\tau_v^+ \\
\partial w/\partial t &= \Theta(u_c - u)(1-w)\tau_w^- - \Theta(u-u_c)w\tau_w^+ \\
J_{fi} &= -v\Theta(u_c - u)(1-u)(u_c - u)/\tau_d \\
J_{so} &= u\Theta(u_c - u)/\tau_o + \Theta(u-u_c)/\tau_r \\
J_{si} &= -g_{si} w(1+\tanh[k(u-u_c^{si})])/2\tau^{si} \\
y_\infty &= (1+e^{(u+1.1)/0.01})^{-1} \\
\tau_h &= 35/[e^{-0.15(u+11)} + e^{50(u-5)}] \\
\partial y/\partial t &= (y_\infty - y)/\tau_h \\
J_h &= S[1.5\,y(u-1) + 1.2\,y(u-u_c)]
\end{aligned}
\qquad (1)
$$

where y is the activation gate for J_h, y_∞ is the steady state of y, τ_h is the voltage dependent time constant of y [4]. D is the diffusion constant representing intercellular gap junctional coupling. When simulating isolated SAN or atrial cell APs, D is given a value 0 mm^2/ms. S is given a value of 0 when simulating atrial AP, and 1 while simulating SAN AP. The time variable was taken to have the units of milliseconds (ms), and the space variable the units of millimeters (mm). The scaled currents J_{fi}, J_{si}, J_{so} and J_h have units of ms^{-1}. All other variables are dimensionless [7]. The cell model specific values of parameters are given in Table 1 of the Appendix.

To develop mouse atrial and SAN AP cell models, parameters of Eq. (1) were optimised with D= 0 mm^2/ms using a procedure similar to the one described in [9]. To allow for rapid optimization, all the basal FK parameters (Table 1) were simultaneously and randomly varied in a ±200% range and a population of 10^4 parameter combinations (inputs) used to produce the corresponding AP properties of APD_{90}, cycle length, resting potential, and maximum potential (outputs). The inputs were then selected which produced outputs close to the required ones, and optimal parameters identified. Two separate parameter optimizations one each for atrial and SAN AP were carried out. As shown in [9], the optimized sets of parameters obtained this way cannot be guaranteed to be unique. However, in our present case all sets producing appropriate outputs happened to be very close to each other. The simulated atrial and SAN APs were validated by comparison with experimental data from mouse isolated cell measurements. The ODEs were integrated using Euler solver at a constant time step of 0.01 ms. The space step in the 1D and 2D models was taken to be 0.1 mm. A finite difference solver using a standard 3 point stencil (1D) and 5 point stencil (2D) was used to obtain numerical solutions of Eq. (1).

To estimate the diffusion constant that gave an experimentally observed atrial conduction velocity of 0.6 mm/ms [10], 1D models consisting of 60 atrial cells and an inter-cellular spacing of 0.1 mm were constructed. Stimuli at a pacing cycle length of 295 ms were applied at one end consisting of a liminal patch of 6 cells that gave rise to stable propagations. The diffusion constant was thus estimated to be 0.028 which gave stable conductions with a CV of 0.6 mm/ms in the 1D model.

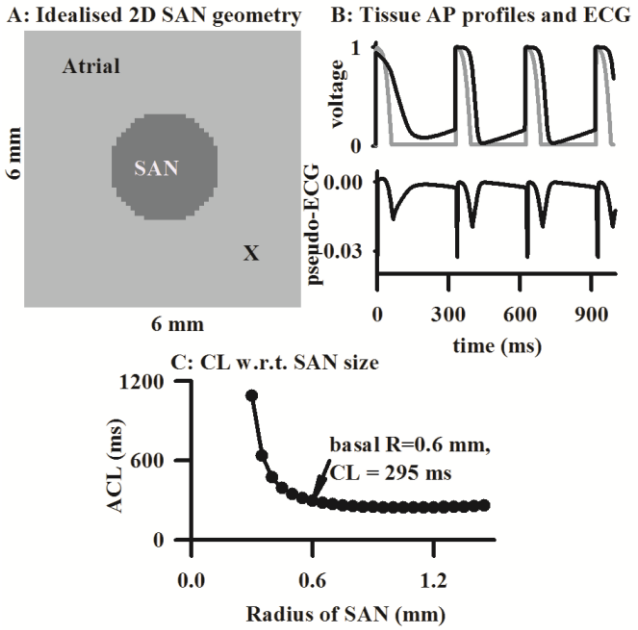

Fig. 2. 2D mouse atrial model. A: 2D model with a central SAN region and surrounding atrial tissue. Atrial AP profile recording site is shown with "X". ACL was computed based on AP recordings at "X". B: Top panel shows AP recordings from SAN region (solid line) and atrial region (gray line) in the 2D model. Bottom panel is the simulated pseudo-ECG. ACL was confirmed using pseudo-ECG. C: ACL as a function of SAN size. The physiological SAN size was found to have a radius (R) of 0.6 mm which gave an ACL of 295 ms.

The two cell types and the diffusion constant were then incorporated into an electrically heterogeneous 2D model. It consisted of a central pacemaking SAN circular region surrounded by an excitable atrial region (Fig 2A). Such a heterogeneous 2D model was encoded into the cardiac geometry format of the Beatbox simulation package which contains location specific cell type information. The size of the 2D model was taken to be 6 mm x 6 mm. A total of 10 s of electrical activity was simulated in each 2D simulation, which took 10 minutes on a standard desktop PC in serial mode.

To quantify the electrical activity in the 2D model, AP profiles were recorded from representative sites in the SAN and atrial region. One such atrial recording site is shown in Fig. 2A. Further, a pseudo-ECG was computed to capture the overall behaviour of the electrical activity in the virtual 2D atrial model. The modified FK kinetics modules that simulated SAN and atrial APs were incorporated into the simulation package. To facilitate visualization of the 2D simulations, a new parallel output module to give VTK files was implemented. The new output module records frames from any 2D simulation at a user defined sampling rate. This output is in binary format and can be rapidly visualized using popular visualization packages like ParaView [11]. A new module that computes pseudo-ECG [12] was also implemented. In this study, the pseudo-ECG lead was assumed to be 2 mm above the center of the 2D model.

In the first set of simulations, the size of the circular SAN region was varied and its effects on atrial pacing quantified. Atrial pacing was quantified by means of plotting SAN size *vs* atrial pacing cycle length (ACL). The SAN size of 0.6 mm that gave the basal ACL of 295 ms was identified and used in the apoptosis simulations.

In the simulations considering cell apoptosis, the SAN size was maintained at a radius of 0.6 mm. However, the fraction of apoptotic cells randomly distributed in the SAN region was altered randomly. An apoptotic cell was defined as a location in the model that neither supported propagation ($D = 0$), nor produced an AP. The fraction of apoptotic cells was increased from 0% to 10% of the total number of SAN cells. As the distribution of apoptotic cells was random in the SAN region, 50 simulations were carried out for each fraction value of apoptotic cell numbers. 50 simulations were deemed to give statistically significant results. Sinus arrest was defined as failure of SAN to initiate electrical propagation into the atrial part of the model. The effects of apoptosis on ACL were quantified by plotting the average ACL *vs* apoptotic cell fraction. At each value of apoptotic cell number, the incidence of sinus arrest was quantified by counting the number of failed propagations in each set of 50 simulations for any given value of apoptotic cell number.

III. Results

The optimised FK model parameters reproduce the experimentally measured mouse atrial AP profiles, with an AP duration (APD_{90}) between 30 and 60 ms [13]. The modified parameters produce an APD_{90} of 50 ms. In the SAN pacemaking AP, the modeling parameters give a pacemaking AP of cycle length 295 ms which is in the range of experimental measurements [4]. The model AP profiles, comparison of APD_{90} and CL to experimental data are shown in Fig. 1. Values of parameters that simulate atrial AP as well as SAN AP used in this study are given in the Appendix Table. Admittedly, the parameters sets thus obtained are not guaranteed to be unique. However, in addition to giving isolated cell excitations of appropriate duration, these parameters allowed simulation of physiological pacemaking in the 1D and 2D tissue models.

The effects of altering SAN size are illustrated in Fig. 2. A larger sized SAN gave rapid atrial pacing while a smaller SAN gave slower pacing rates. For large SAN size, the ACL was approximately 280 ms and did not reduce with increasing of SAN size. For a SAN size with radius 0.6 mm, a physiological ACL of 295 ms was obtained. Therefore, this was taken to be the estimate of basal SAN size. Such an estimate is in agreement with experimental measurements where SAN size was determined by HCN4 fluorescence mapping [14]. A progressive reduction of SAN size led to a progressive reduction of atrial pacing rates. For SAN radius less than 0.5 mm, atrial pacing was arrested. In addition to arresting atrial pacing, the SAN region also failed to produce pacemaking excitations due to electrotonic loading of SAN by the surrounding atria tissue.

A representative simulation involving 3% pacemaker cell apoptosis is illustrated in Fig. 3. Fig. 3A shows a representative 2D geometry where atrial, SAN pacemaker,

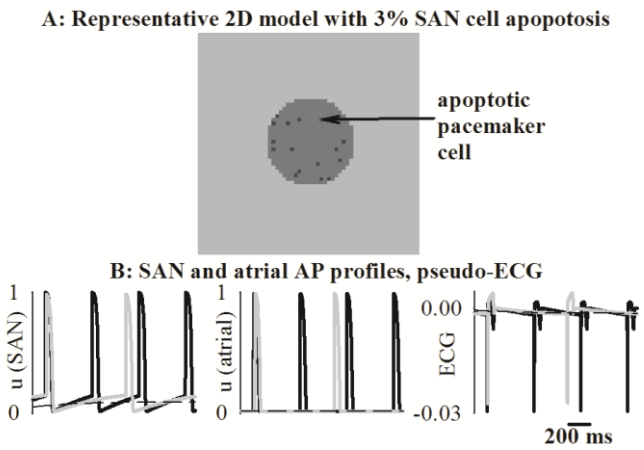

Fig. 3. A: Atrial (light gray), SAN (dark gray), and apoptotic cells (black) in the 2D idealized model. B: Representative SAN APs (left panel), atrial APs (middle panel), and pseudo-ECG profiles from the 3% apoptosis simulation. Out of the 50 run population, the APs shown are ACL = 400 ms (black lines in all 3 panels), ACL = 800 ms (gray lines), and a SAN arrest case (dashed black lines).

and randomly distributed apoptotic cells are present. 50 such geometries involving 3% apoptotic cells were generated, and 2D simulations conducted using each. A sizable fraction of these 50 computations showed that the SAN was capable of driving the atrial tissue. However, the ACL with which atrial tissue was paced varied markedly. The variations are reflected in the SAN and atrial AP recordings, as well as from the pseudo-ECG. In some cases, 3% apoptosis caused a total sinus arrest. Similar to the 3% pacemaker cell apoptosis simulation, a number of simulations were carried out for pacemaker cell apoptosis between 0% and 10%. Analysis of the results is illustrated in Fig. 4. For a low fraction of apoptotic cells the atrial pacing rates, quantified by the average ACL, were close to physiological rates. The standard deviation of ACL obtained from the population of 50 simulations was small, indicating that a small number of apoptotic cells do not affect the periodic pacemaking SAN function. However, as the fraction of apoptotic cells was increased, we observed that: a) as seen in Fig. 4A, the ACL increased as the fraction of apoptotic cells increased. This indicates increasing bradycardia; b) the variability of ACL increased dramatically as the fraction of apoptotic cells increased, which indicates the increased variability of pacing. It also reflects the increased recovery time of the SAN, and our simulations correlate the recovery time to cell apoptosis without altering any other electrophysiology; and c) as seen in Fig. 4B, the number of cases in each population of 50 runs where propagation failed increased, i.e. the incidence of sinus arrest increased. This was accompanied by neither atrial pacing nor pacemaker AP excitation.

The level of apoptosis required to cause a total sinus arrest was 9%. The rate at which the SAN paced the atrial tissue can be seen to be correlated to the exact and sub-geometry of the apoptotic cells in the SAN region. It should be noted that we never observed the case where the SAN produced excitations that did not propagate. When there was a SAN

excitation, it propagated. Thus the model is limited in that it cannot produce sinus pause or exit block.

IV. Conclusion

The phenomenological FK model succinctly captures all the important features of generic electrophysiological excitable systems while being computationally efficient. It is capable of producing mouse atrial AP profiles suitable for computational experiments. It has been extended to include cell membrane pacemaking mechanisms like the hyperpolarisation activated current to simulate mouse SAN pacemaking. Using these cell types in spatially extended models, this study shows the importance of SAN size for physiological pacemaking function. Importantly, simulation of disease related apoptosis in the model allows the estimation of alterations on atrial pacemaking and the occurrence of bradycardia. A classic feature of SND being sinus pause could not be simulated using models presented in this study. This limitation of the model is due to the lack of intracellular Ca^{2+} mechanisms. In future studies, such mechanisms will be considered to extend the modeling capability. Notwithstanding, the 2 cell types and the 2D model developed were able to reproduce bradycardia and sinus arrest conditions. The presented models are suitable for preliminary studies into mouse atrial electrophysiology and electrical propagation behaviour.

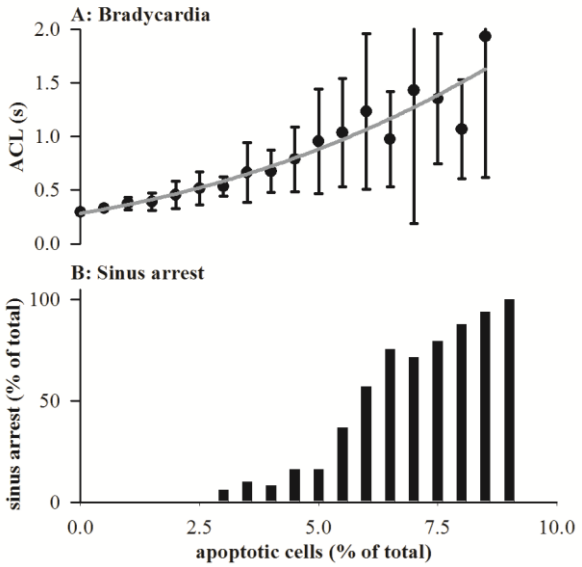

Fig. 4. Bradycardia and sinus arrest in SAN consisting of apoptotic cells. The horizontal axis for both panels is shown in panel B. A: Increase of average ACL as the fraction of apoptotic cells is increased. The dots show the mean ACL value, error bars show the standard deviation of ACL, and the gray line shows a best fit to the simulation data. B: Increased incidence of sinus arrest or conduction failure as fraction of apoptotic cells is increased.

V. Appendix

Table 1. Parameters for the FK, atrial, and SAN AP models.

	u_c	u_v	τ_d	τ_0	τ_{si}	τ_r	τ_v^+
FK	0.13	0.04	0.25	12.5	30	33	3.33
atrial	0.01	0.04	0.25	5	100	21	3.33
SAN	0.2	0.5	0.05	16.5	45	115	16.5

	τ_v^-	τ_w^+	τ_w^-	u_c^{si}	k	g_{si}
FK	1250	870	41	0.85	1	0.5
atrial	1250	870	41	0.95	0.001	0.5
SAN	12000	1.5	400	0.01	2.5	2

References

[1] H. Dobrzynski, M. R. Boyett, and R. H. Anderson, "New insights into pacemaker activity: promoting understanding of sick sinus syndrome," *Circulation,* vol. 115, pp. 1921-32, Apr 10 2007.

[2] M. E. Mangoni, A. Traboulsie, A. L. Leoni, B. Couette, L. Marger, K. Le Quang, E. Kupfer, A. Cohen-Solal, J. Vilar, H. S. Shin, D. Escande, F. Charpentier, J. Nargeot, and P. Lory, "Bradycardia and slowing of the atrioventricular conduction in mice lacking CaV3.1/alpha1G T-type calcium channels," *Circ. Res.,* vol. 98, pp. 1422-30, Jun 9 2006.

[3] M. Lei, H. Zhang, A. A. Grace, and C. L. Huang, "SCN5A and sinoatrial node pacemaker function," *Cardiovasc. Res.,* vol. 74, pp. 356-65, Jun 1 2007.

[4] S. Kharche, J. Yu, M. Lei, and H. Zhang, "A mathematical model of action potentials of mouse sinoatrial node cells with molecular bases," *Am J Physiol Heart Circ Physiol,* vol. 301, pp. H945-63, Sep 2011.

[5] E. G. Lakatta, V. A. Maltsev, and T. M. Vinogradova, "A coupled SYSTEM of intracellular Ca2+ clocks and surface membrane voltage clocks controls the timekeeping mechanism of the heart's pacemaker," *Circ Res,* vol. 106, pp. 659-73, Mar 5 2010.

[6] P. D. Swaminathan, A. Purohit, S. Soni, N. Voigt, M. V. Singh, A. V. Glukhov, Z. Gao, B. J. He, E. D. Luczak, M. L. Joiner, W. Kutschke, J. Yang, J. K. Donahue, R. M. Weiss, I. M. Grumbach, M. Ogawa, P. S. Chen, I. Efimov, D. Dobrev, P. J. Mohler, T. J. Hund, and M. E. Anderson, "Oxidized CaMKII causes cardiac sinus node dysfunction in mice," *J Clin Invest,* vol. 121, pp. 3277-88, Aug 2011.

[7] F. Fenton and A. Karma, "Vortex dynamics in three-dimensional continuous myocardium with fiber rotation: Filament instability and fibrillation," *Chaos,* vol. 8, pp. 20-47, Mar 1998.

[8] R. McFarlane and I. V. Biktasheva, "Beatbox—A Computer Simulation Environment for Computational Biology of the Heart," in *Visions of Computer Science— BCS International Academic Conference*, London, 2008, pp. 99-109.

[9] S. Kharche, N. Ludtke, S. Panzeri, and H. Zhang, *A Global Sensitivity Index for Biophysically Detailed Cardiac Cell Models: A Computational Approach* vol. 5528, 2009.

[10] D. E. Leaf, J. E. Feig, C. Vasquez, P. L. Riva, C. Yu, J. M. Lader, A. Kontogeorgis, E. L. Baron, N. S. Peters, E. A. Fisher, D. E. Gutstein, and G. E. Morley, "Connexin40 imparts conduction heterogeneity to atrial tissue," *Circ Res,* vol. 103, pp. 1001-8, Oct 24 2008.

[11] A. Henderson, *ParaView Guide, A Parallel Visualization Application.*: Kitware Inc., 2007.

[12] K. Gima and Y. Rudy, "Ionic current basis of electrocardiographic waveforms: a model study," *Circ Res,* vol. 90, pp. 889-96, May 3 2002.

[13] A. E. Lomax, C. S. Kondo, and W. R. Giles, "Comparison of time- and voltage-dependent K+ currents in myocytes from left and right atria of adult mice," *Am J Physiol Heart Circ Physiol,* vol. 285, pp. H1837-48, Nov 2003.

[14] S. Herrmann, J. Stieber, G. Stockl, F. Hofmann, and A. Ludwig, "HCN4 provides a 'depolarization reserve' and is not required for heart rate acceleration in mice," *EMBO. J.,* vol. 26, pp. 4423-32, Oct 31 2007.